University of California

Los Angeles

Closed-Loop Subspace Identification of a Quadrotor

A thesis submitted in partial satisfaction

of the requirements for the degree

Master of Science in Engineering

by

Andrew G. Kee

2013

Abstract of the Thesis

Closed-Loop Subspace Identification of a Quadrotor

by

Andrew G. Kee

Master of Science in Engineering

University of California, Los Angeles, 2013

Professor Steve Gibson, Chair

Ne quo feugiat tractatos temporibus, eam te malorum sensibus. Impetus voluptua senserit id mel, lucilius adipiscing at duo. Suas noster sanctus cu pro, movet dicam intellegebat pri ad, esse utamur vulputate ut per. Admodum facilisi sea an, omittam molestiae pertinacia vim eu, et eam illud graeco. Enim persius duo ei, mea te posse congue putent.

Has ut commodo inermis definiebas. Eu pro audire fabellas. Te qui zril omnes forensibus, ius an dico tempor maiorum. Ea mel illud adipisci.

Ad vel dicant aliquip, ut eam agam constituto, no quo erant melius. Porro labores invidunt ad vel, quaeque epicurei vituperatoribus ex cum. Qui tamquam omnesque ex, essent percipitur intellegam an per. Iusto expetenda sed et.

The thesis of Andrew G. Kee is approved.

Steve Gibson, Committee Chair

University of California, Los Angeles

2013

Table of Contents

List of Figures

List of Tables

Nomenclature

$\mathbb{R}$	Set of all reals
$\mathbb{Z}$	Set of all integers
A	System matrix
B	Input matrix
C	Output matrix
D	Feedforward matrix
u	System input vector
y	System output vector
e	System innovation vector
x	System state vector
v	Process noise vector
w	Measurement noise vector
n	Number of system states
m	Number of system inputs
l	Number of system outputs
l	Number of system outputs
σ	Singular value
K	Kalman filter gain
U_k	Block Hankel matrix of system inputs
U_p	Block Hankel matrix of past system inputs
U_f	Block Hankel matrix of future system inputs
Y_k	Block Hankel matrix of system outputs
Y_p	Block Hankel matrix of past system outputs
Y_f	Block Hankel matrix of future system outputs
X_k	Block Hankel matrix of system states

E_k	Block Hankel matrix of system innovation
E_f	Block Hankel matrix of future system innovation
Γ_k	Extended observability matrix
$\hat{\Gamma}_f$	Estimate of extended observability matrix over future horizon
G_f	Toeplitz matrix of future Markov parameters of stochastic subsystem
H_f	Toeplitz matrix of future Markov parameters of deterministic subsystem
f	Future time horizon
p	Past time horizon
$\Pi_{U_f}^{\perp}$	Orthogonal projection onto the column space of U_f
I	Identity matrix
Z	Instrumental variable matrix
Z_p	Instrumental variable matrix constructed of past input-output data
ϕ	Pitch
θ	Roll
$\dot{\psi}$	Yaw rate

CHAPTER 1

Introduction

Unmanned Aerial Vehicles (UAVs) have seen explosive growth in the past thirty years, performing a multitude of military and civilian tasks including surveillance, reconnaissance, armed combat operations, search and rescue, forest fire management, and domestic policing [15, 17]. A class of modern UAVs which have recently grown in popularity are quadrotors - Vertical Take Off and Landing (VTOL) vehicles powered by four rotors arranged in a cross configuration. The main advantage of the quadrotor lies in its mechanical simplicity. Adjusting the speed of one or more of the vehicle's fixed-pitch rotors provides full attitude control, eliminating the need for the swash plate mechanism found on single rotor helicopters [2, 4]. In spite of its mechanical simplicity, the quadrotor exhibits somewhat complex dynamics that are best modeled as a Multi-Input Multi-Output (MIMO) system.

Advances in MEMS sensors and light-weight high-powered lithium polymer batteries have contributed to the recent popularity of quadrotors, making them an attractive choice for research applications in flight dynamics and control, as in [5, 9, 11, 12]. One problem of particular interest is the development of mathematical models representing system dynamics based on experimentally gathered data. System identification provides a mechanism to relate this input-output data to the underlying system dynamics. Traditionally, system identification techniques have focused on developing a system model which minimizes prediction error. Identification methods of this form are commonly known as Prediction Error Methods (PEMs). PEMs have seen widespread use in both theoretical and real-world applications, but experience difficulties with MIMO systems as noted in [13, 23]. Subspace identification methods have recently grown in popularity and offer an alternative approach to the identification problem. These methods have a foundation in linear algebra and overcome the issues found in PEMs when identifying MIMO systems [8]. It is the goal of this research project to apply subspace identification techniques to a quadrotor using experimentally gathered closed-loop input and output data.

1.1 Related Work

1.2 Motivation and Contributions

CHAPTER 2

Preliminaries

2.1 Notation

Let $\mathbb{R}$ be the set of reals, $\mathbb{R}^n$ the set of n-dimensional real vectors, and $\mathbb{R}^{m\times n}$ the set of real matrices. We denote vectors by lower case letters $\{a,\ b,\ c,\ \ldots\}$ and matrices by upper case letters $\{A,\ B,\ C,\ \ldots\}$. Transpositions of vectors and matrices are denoted by a^T and A^T, respectively. The inverse of a square matrix A is denoted A^{-1} and its Moore-Penrose psedudoinverse is denoted by $A^\dagger$.

2.2 Linear Systems

2.2.1 Linear Time-Invariant Systems

A discrete time state space representation of a linear dynamical system can be written as

$$x(k+1) = Ax(k) + Bu(k) \tag{2.1a}$$

$$y(k) = Cx(k) + Du(k) \tag{2.1b}$$

where $x(k) \in \mathbb{R}^n$ is a vector of the states of the system, $u(k) \in \mathbb{R}^m$ is a vector of input signals, and $y(k) \in \mathbb{R}^l$ is a vector of output signals for $k \in \mathbb{Z}$. A, B, C, and D are the system matrices with dimensions $A \in \mathbb{R}^{n\times n}$, $B \in \mathbb{R}^{n\times m}$, $C \in \mathbb{R}^{l\times n}$, $D \in \mathbb{R}^{l\times m}$.

It is important to see that the system state is not unique. That is, there are different state space representations resulting in the same input-output behavior

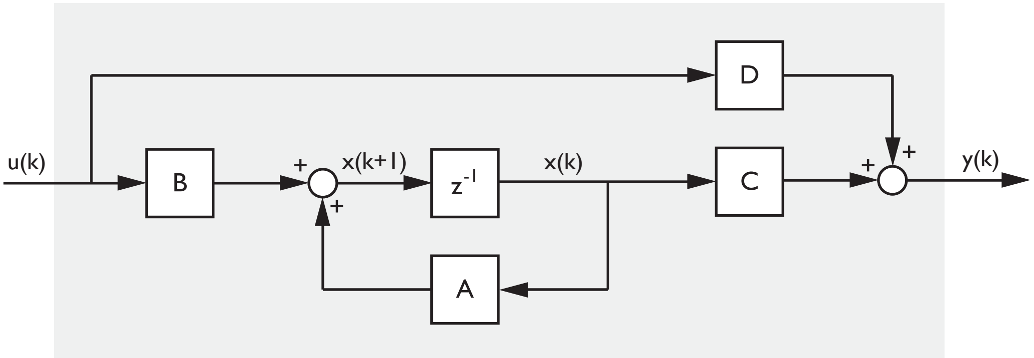

Figure 2.1: A block diagram of the state space representation of an LTI system.

of the system. These differing states can be related by a similarity transform T where T is a real, nonsingular matrix:

$$\tilde{x}(k) = T^{-1}x(k)$$

The state space representation of the system corresponding to the transformed state $\tilde{x}$ is given by

$$\tilde{x}(k+1) = \tilde{A}\tilde{x}(k) + \tilde{B}u(k)$$

$$y(k) = \tilde{C}\tilde{x}(k) + \tilde{D}u(k)$$

with

$$\tilde{A} = T^{-1}AT, \qquad \tilde{B} = T^{-1}B, \qquad \tilde{C} = CT, \qquad \tilde{D} = D$$

2.2.2 Stability

The LTI system given by A, B, C, D is said to be *stable* if all the eigenvalues of A lie strictly within the unit circle on the complex plane.

2.2.3 Observability and Controllability

The LTI system given by A, B, C, D or equivalently the pair (A, C) is said to be *observable* if for any finite time $t_1 > 0$, the initial state $x(0) = x_0$ can be uniquely determined from measurements of the input u and output y over the interval $[0, t_1], t_1 > 0$.

The LTI system given by A, B, C, D or equivalently the pair (A, B) is said to be *controllable* if for any final state x_1 there exists an input sequence u_k defined on the interval $[0, t_1], t_1 > 0$ that transfers the state from $x(0) = x_0$ to x_1 in finite time.

LTI systems A, B, C, D in state space form which are both observable and controllable are said to be *minimal*, meaning that the matrix A has the smallest possible dimension.

2.2.4 Combined Deterministic-Stochastic LTI Systems

Section 2.2.1 considered the case of a purely deterministic system; that is, a system operating in a noise-free environment. In practice, this rarely happens so we will now consider the case of the combined deterministic-stochastic LTI system operating in the presence of process and measurement noise. We append 2.1 as follows

$$x(k+1) = Ax(k) + Bu(k) + w(k) \tag{2.3a}$$

$$y(k) = Cx(k) + Du(k) + v(k) \tag{2.3b}$$

where $w(k) \in \mathbb{R}^1$ and $v(k) \in \mathbb{R}^1$ are the process and measurement noises, respectively. As is commonly done, we assume $w(k)$ and $v(k)$ are zero-mean white-noise sequences.

If the system is observable, we can design a Kalman filter to estimate the system state [7]

$$\hat{x}(k+1) = A\hat{x}(k) + Bu(k) + K\big(y(k) - C\hat{x}(k) - Du(k)\big)$$

where K is the Kalman filter gain. If we denote

$$e(k) = y(k) - C\hat{x}(k) - Du(k)$$

to be the innovation sequence, we can rewrite the combined deterministic-stochastic system in Eq. (2.3) in the following equivalent *innovation form*:

$$x(k+1) = Ax(k) + Bu(k) + Ke(k) \tag{2.4a}$$

$$y(k) = Cx(k) + Du(k) + e(k) \tag{2.4b}$$

We will use the state space model in its innovation form to describe the subspace algorithm for identifying both open and closed-loop combined deterministic-stochastic LTI systems.

2.3 Linear Algebra Tools

2.3.1 Fundamental Matrix Subspaces

We require two of the fundamental matrix subspaces: the column space and the row space. The column space of a matrix $A \in \mathbb{R}^{m \times n}$ is the set of all linear combinations of the column vectors of A, sometimes called the range of A. The dimension of the column space is called the rank. The row space of a matrix $A \in \mathbb{R}^{m \times n}$ is the set of all linear combinations of the row vectors of A.

2.3.2 Orthogonal Projections

The *orthogonal projection* of the row space of A onto the row space of B is $A\Pi_B$, defined as

$$A\Pi_B = AB^T(BB^T)^{-1}B$$

The projection of the row space of A onto the orthogonal compliment of the row space of B is $A\Pi_B^{\perp}$, defined as

$$A\Pi_B^{\perp} = A\big(I - B^T(BB^T)^{-1}B\big)$$

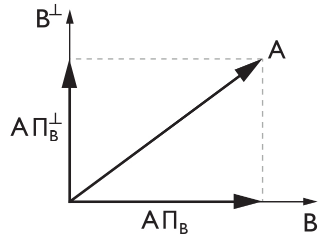

Figure 2.2: Orthogonal projections.

Additionally, we define the following properties of orthogonal projections:

$$B\Pi_B = BB^T(BB^T)^{-1}B = B$$

$$B\Pi_B^{\perp} = B\big(I - B^T(BB^T)^{-1}B\big) = B - B = 0$$

When B is large, computing its inverse and thus orthogonal projections onto its subspaces is computationally intensive. A more numerically efficient computation of of an orthogonal projection is achieved by LQ decomposition. From the LQ decomposition,

$$\begin{bmatrix} B \\ A \end{bmatrix} = \begin{bmatrix} L_{11} & 0 \\ L_{21} & L_{22} \end{bmatrix} \begin{bmatrix} Q_1 \\ Q_2 \end{bmatrix}$$

we have

$$A\Pi_B = L_{21}Q_1$$

$$A\Pi_B^{\perp} = L_{22}Q_2$$

2.3.3 Singular Value Decomposition

Any matrix $A \in \mathbb{R}^{m\times n}$ can be decomposed by a singular value decomposition (SVD) given by

$$A = U\Sigma V^T$$

where $U \in \mathbb{R}^{m\times m}$ and $V \in \mathbb{R}^{n\times n}$ are orthogonal matrices and $\Sigma \in \mathbb{R}^{m\times n}$ is diagonal matrix of the singular values σ_i of A ordered such that

$$\sigma_1 \geq \sigma_2 \geq \cdots \geq \sigma_r > 0$$

If we partition the matrices in the SVD as

$$A = \left[\begin{array}{c|c} U_1 & U_2 \end{array}\right] \left[\begin{array}{c|c} \Sigma_r & 0 \\ \hline 0 & 0 \end{array}\right] \left[\begin{array}{c} V_1^T \\ \hline V_2^T \end{array}\right]$$

a well known property of the SVD is that the vectors U_1 corresponding to the r non-zero singular values of A span the range of A. That is,

$$\text{range}(U_1) = \text{range}(A)$$

We will later use this property to recover an estimate of the column space (range) of the extended observability matrix from input-output data.

2.3.4 Hankel Matrices

A Hankel matrix is a matrix $A \in \mathbb{R}^{m \times n}$ with constant skew-diagonals:

$$A_{m,n} = \begin{bmatrix} a_1 & a_2 & \cdots & a_n \\ a_2 & a_3 & \cdots & a_{n+1} \\ \vdots & \vdots & \ddots & \vdots \\ a_m & a_{m+1} & \cdots & a_{m+n-1} \end{bmatrix}$$

Hankel matrices can be constructed by setting the i, j^{th} element of A to

$$A_{i,j} = A_{i-1,j+1}$$

If each entry in the matrix is also a matrix, the resulting matrix is called a block Hankel matrix:

2.3.5 Toeplitz Matrices

A Toeplitz matrix is a matrix $A \in \mathbb{R}^{m \times n}$ with constant diagonals.

$$A_{m,n} = \begin{bmatrix} a_1 & a_{-1} & \cdots & a_{-n+1} \\ a_2 & a_1 & \ddots & \vdots \\ \vdots & \ddots & \ddots & a_{-1} \\ a_{m-1} & \cdots & a_2 & a_1 \end{bmatrix}$$

Topelitz matrices can be constructed by setting the i, j^{th} element of A to

$$A_{i,j} = A_{i+1,j+1}$$

CHAPTER 3

Subspace Identification Methods

Subspace identification methods (SIM) provide an approach to identifing LTI systems in their state space form using input-output data. SIMs provide an attractive alternative to Prediction Error Methods (PEM) because of their ability to identify MIMO systems and their non-iterative solution nature, making them suitable for working with large data sets. In general, the subspace identification problem is: given a set of input and output data, estimate the system matrices (A, B, C, D) up to within a similarity transform.

Extensive work in both the theory and application of SIMs in the last 20 years has resulted in the development of a number of popular algorithms, including the canonical variate analysis (CVA) method proposed by Larimore [10], the multi-variable output-error state space (MOESP) method proposed by Verhaegen [21], and the numerical algorithms for subspace state space system identification (N4SID) proposed by Van Overschee and De Moor [18]. A unifying theorem subsequently proposed by Van Overschee and De Moor [19] links these algorithms and provides a generalized approach to the subspace identification problem.

As described in Van Overschee and De Moor's unifying theorem, all SIMs follow the same general two step procedure. First, estimate the subspace spanned by the columns of the extended observability matrix (Γ_k) from input-output data u_k, y_k. Because the dimension of Γ_k determines the order n of the estimated system, a reduction of the system order is performed before proceeding. Second, the system matrices are determined, either directly from the extended observability matrix or from the realized state sequence X_k.

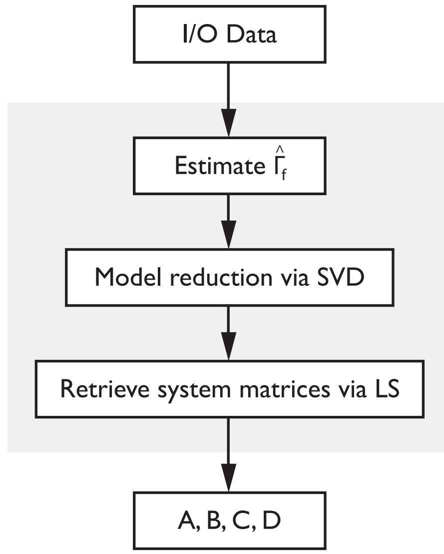

Figure 3.1: Subspace identification approach

3.1 Subspace System Identification

First, we consider the identification of a combined deterministic-stochastic LTI system operating in open loop. We present an overview of the PO-MOESP sub-

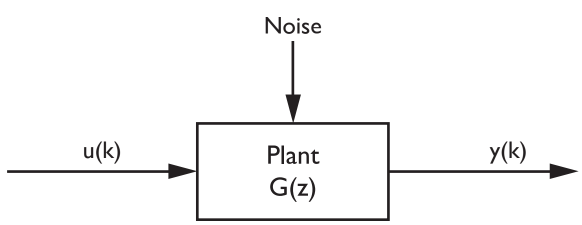

Figure 3.2: A block diagram of an LTI system operating in open loop.

space identification procedure, where "PO" indicates that both past input and output data is used when eliminating the influence of noise on the identified system. Before detailing the identification procedure, we introduce the following assumptions:

Assumption 1: The matrix $A - KC$ is stable (i.e. its eigenvalues lie strictly within the unit circle).

Assumption 2: The pair (A, C) is observable and $(A, [B \quad K])$ is observable.

Assumption 3: The innovation sequence $e(k)$ is zero-mean white noise.

Assumption 4: The input sequence $u(k)$ and innovation sequence $e(k)$ are uncorrelated for all k.

Assumption 5: The input sequence $u(k)$ is persistently exciting.

3.1.1 Extended State Space Model

Recalling the combined deterministic-stochastic LTI system is given in its innovation form as

$$x(k+1) = Ax(k) + Bu(k) + Ke(k) \tag{3.1a}$$

$$y(k) = Cx(k) + Du(k) + e(k) \tag{3.1b}$$

Based on the state space representation, an extended state space model can be formulated as

$$Y_p = \Gamma_p X_{k-p} + H_p U_p + G_p E_p \tag{3.2a}$$

$$Y_f = \Gamma_f X_k + H_f U_f + G_f E_f \tag{3.2b}$$

where p and f denote past and future horizons, respectively. The extended observability matrix is

$$\Gamma_f = \begin{bmatrix} C \\ CA \\ \vdots \\ CA^{f-1} \end{bmatrix}$$

and H_f and G_f are Toeplitz matrices of the Markov parameters of the deterministic and stochastic subsystems, respectively:

$$H_f = \begin{bmatrix} D & 0 & 0 & \cdots & 0 \\ CB & D & 0 & \cdots & 0 \\ CAB & CB & D & \cdots & 0 \\ \vdots & \vdots & \vdots & \ddots & \vdots \\ CA^{f-2}B & CA^{f-3}B & CA^{f-4}B & \cdots & D \end{bmatrix}$$

$$G_f = \begin{bmatrix} I & 0 & 0 & \cdots & 0 \\ CK & I & 0 & \cdots & 0 \\ CAK & CK & I & \cdots & 0 \\ \vdots & \vdots & \vdots & \ddots & \vdots \\ CA^{f-2}K & CA^{f-3}K & CA^{f-4}K & \cdots & I \end{bmatrix}$$

We arrange the input sequence into the following block Hankel form with k block rows and N columns:

$$U_p = \begin{bmatrix} u(0) & u(1) & \cdots & u(N-1) \\ u(1) & u(2) & \cdots & u(N) \\ \vdots & \vdots & \ddots & \vdots \\ u(k-1) & u(k) & \cdots & u(k+N-2) \end{bmatrix}$$

$$U_f = \begin{bmatrix} u(k) & u(k+1) & \cdots & u(k+N-1) \\ u(k+1) & u(k+2) & \cdots & u(k+N) \\ \vdots & \vdots & \ddots & \vdots \\ u(2k-1) & u(2k) & \cdots & u(2k+N-2) \end{bmatrix}$$

We construct similar matrices Y_p, Y_f, E_p, and E_f for the output and noise sequences. The state sequences are

$$X_k = \begin{bmatrix} x(k) & x(k+1) & \cdots & x(k+N-1) \end{bmatrix}$$

$$X_{k-p} = \begin{bmatrix} x(k-p) & x(k-p+1) & \cdots & x(k-p+N-1) \end{bmatrix}$$

We will leverage this structure of the extended state space model to identify the unknown system matrices from known input-output data. In particular, we will estimate the column space of the extended observability matrix. Knowledge of this subspace is sufficient to then recover the unknown system matrices.

3.1.2 Estimation of the Extended Observability Matrix

Determination of the system matrices relies on an estimate of the column space of Γ_f. Recalling the extended state space model and considering only the future horizon, we have

$$Y_f = \Gamma_f X_k + H_f U_f + G_f E_f \tag{3.3}$$

In order to estimate the column space of Γ_f in Eq. (3.3), we must eliminate the influence of the input and noise terms. The general procedure, as outlined in [13, 22] is as follows: First, we eliminate the influence of the input U_f by post-multiplying Eq. (3.3) by $\Pi^{\perp}_{U_f}$ where $\Pi^{\perp}_{U_f}$ is an orthogonal projection onto the column space of U_f given by

$$\Pi^{\perp}_{U_f} = I - U_f^T (U_f U_f^T)^{-1} U_f$$

By definition, $U_f \Pi^{\perp}_{U_f} = 0$ so Eq. (3.3) becomes

$$Y_f \Pi^{\perp}_{U_f} = \Gamma_f X_k \Pi^{\perp}_{U_f} + G_f E_f \Pi^{\perp}_{U_f} \tag{3.4}$$

By Assumption 4, E_f is uncorrelated with U_f. That is,

$$E_f \Pi^{\perp}_{U_f} = E_f (I - U_f^T (U_f U_f^T)^{-1} U_f) = E_f$$

so

$$Y_f \Pi^{\perp}_{U_f} = \Gamma_f X_k \Pi^{\perp}_{U_f} + G_f E_f \tag{3.5}$$

Next we eliminate the influence of the noise E_f. In order to remove the influence of the noise on the extended observability matrix, we must introduce an instrumental variable matrix as described in [22]. We seek a matrix $Z \in \mathbb{R}^{2k \times N}$ which exhibits the following properties:

$$\lim_{N\to\infty} \frac{1}{N} E_f Z^T = 0 \tag{3.6a}$$

$$\text{rank}\left(\lim_{N\to\infty} \frac{1}{N} X_k \Pi_{U_f}^{\perp} Z^T\right) = n \tag{3.6b}$$

Satisfying condition (3.6a) ensures that we can eliminate E_f by multiplying Eq. (3.5) on the right by Z^T and taking the limit for $N \to \infty$:

$$\lim_{N\to\infty} \frac{1}{N} Y_f \Pi_{U_f}^{\perp} Z^T = \lim_{N\to\infty} \frac{1}{N} \Gamma_f X_k \Pi_{U_f}^{\perp} Z^T \tag{3.7}$$

Satisfying condition (3.6b) ensures multiplication by Z does not change the rank of the remaining term on the right hand side of Eq. (3.7) so we have

$$\text{range}\left(\lim_{N\to\infty} \frac{1}{N} Y_f \Pi_{U_f}^{\perp} Z^T\right) = \text{range}\left(\Gamma_f\right) \tag{3.8}$$

From Eq. (3.8) we see that an SVD of the matrix $Y_f \Pi_{U_f}^{\perp} Z^T$ will provide an estimate of the column space of Γ_f. All that remains is to identify a suitable instrumental variable matrix Z. As described in [16, 22], instrumental variable matrices are typically constructed from input-output data. Recalling that we partitioned our input and output data into "past" and "future" sets in Section 3.2.1, we will use the "future" input-output data to identify the system and the "past" input-output data as the instrumental variable matrix Z_p:

$$Z_p = \begin{bmatrix} U_p \\ Y_p \end{bmatrix}$$

Recalling that E_f is uncorrelated with U_f for open-loop systems, and enforcing the assumption that E_f is white-noise, we have from [22] that

$$\lim_{N\to\infty} \frac{1}{N} E_f Z_p^T = 0$$

which satisfies condition (3.6a). Jannson showed in [6] that if the input sequence is persistently exciting (Assumption 5), the rank condition (3.6b) is satisfied. Taking

Z_p as the instrumental variable matrix and taking the SVD, from Eq. (3.8) we have

$$\hat{\Gamma}_f = US^{1/2} \tag{3.9}$$

3.1.3 Rank Reduction

In the presence of noise, the matrix $Y_f \Pi_{U_f}^{\perp} Z_p^T$ is full rank while the true system order is smaller. We choose the order of the identified system by partitioning the SVD matrices as follows:

$$Y_f \Pi_{U_f}^{\perp} Z_p^T = \begin{bmatrix} U_1 & U_2 \end{bmatrix} \begin{bmatrix} S_1 & 0 \\ 0 & S_2 \end{bmatrix} \begin{bmatrix} V_1^T & V_2^T \end{bmatrix}$$

where the number of singular values n in S_1 is equal to the system order and the remaining submatrices are scaled appropriately. The reduced rank estimate of the extended observability matrix is then

$$\hat{\Gamma}_f = U_1 {S_1}^{1/2} \tag{3.10}$$

3.1.4 Determination of the System Matrices

With an estimate of the column space of Γ_f, we are not able to recover the system matrices. In order to recover the system matrices, we follow the general procedure as outlined in [8]. First, we will exploit the structure of the extended observability matrix to recover the A and C matrices. The matrix C can be read directly from the first block row of $\hat{\Gamma}_f$. In order to recover A, we define the following two matrices

$$\hat{\overline{\Gamma}}_f = \begin{bmatrix} C \\ \vdots \\ CA^{f-2} \end{bmatrix}, \qquad \hat{\underline{\Gamma}}_f = \begin{bmatrix} CA \\ \vdots \\ CA^{f-1} \end{bmatrix} \tag{3.11}$$

where $\hat{\overline{\Gamma}}_f$ is equal to $\hat{\Gamma}_f$ without the last block row and $\hat{\underline{\Gamma}}_f$ is equal to $\hat{\Gamma}_f$ without the first block row. The structure of the matrices in Eq. (3.11) implies

$$\hat{\overline{\Gamma}}_f A = \hat{\underline{\Gamma}}_f \tag{3.12}$$

which is linear in A and can be solved by least squares.

All that remains is to recover the B and D matrices. Recalling the extended state space model is given by

$$Y_f = \Gamma_f X_k + H_f U_f + G_f E_f$$

and multiplying on the left by $\hat{\Gamma}_f^{\perp}$ and on the right by ${U_f}^{\dagger}$ we have

$$\hat{\Gamma}_f^{\perp} Y_f {U_f}^{\dagger} = \hat{\Gamma}_f^{\perp} \Gamma_f X_k {U_f}^{\dagger} + \hat{\Gamma}_f^{\perp} H_f U_f {U_f}^{\dagger} + \hat{\Gamma}_f^{\perp} G_f E_f {U_f}^{\dagger} \tag{3.13}$$

where $\hat{\Gamma}_f^{\perp}$ satisfies $\hat{\Gamma}_f^{\perp}\hat{\Gamma}_f = 0$ and $\dagger$ denotes the Moore-Penrose pseudoinverse. Equation (3.13) simplifies to

$$\hat{\Gamma}_f^{\perp} Y_f {U_f}^{\dagger} = \hat{\Gamma}_f^{\perp} H_f \tag{3.14}$$

Partitioning $\hat{\Gamma}_f^{\perp} Y_f {U_f}^{\dagger}$ into columns with the i^{th} column denoted by $\mathcal{M}_i$ and $\hat{\Gamma}_f^{\perp}$ into rows with the j^{th} row denoted by $\mathcal{L}_j$, Eq. (3.14) is

$$\begin{bmatrix} \mathcal{M}_1 & \mathcal{M}_2 & \cdots & \mathcal{M}_f \end{bmatrix} = \begin{bmatrix} \mathcal{L}_1 \\ \mathcal{L}_2 \\ \vdots \\ \mathcal{L}_f \end{bmatrix} \begin{bmatrix} D & 0 & \cdots & 0 \\ CB & D & \cdots & 0 \\ \vdots & \vdots & \ddots & \vdots \\ CA^{f-2}B & CA^{f-3}B & \cdots & D \end{bmatrix}$$

We can rewrite the above equation as

$$\begin{bmatrix} \mathcal{M}_1 \\ \mathcal{M}_2 \\ \mathcal{M}_3 \\ \vdots \\ \mathcal{M}_f \end{bmatrix} = \begin{bmatrix} \mathcal{L}_1 & \mathcal{L}_2 & \cdots & \mathcal{L}_{f-1} & \mathcal{L}_f \\ \mathcal{L}_2 & \mathcal{L}_3 & \cdots & \mathcal{L}_f & 0 \\ \mathcal{L}_3 & \mathcal{L}_4 & \cdots & 0 & 0 \\ \vdots & \vdots & \ddots & \vdots & \vdots \\ \mathcal{L}_f & 0 & 0 & \cdots & 0 \end{bmatrix} \begin{bmatrix} I & 0 \\ 0 & \hat{\overline{\Gamma}}_f \end{bmatrix} \begin{bmatrix} D \\ B \end{bmatrix} \tag{3.15}$$

which is an overdetermined linear system in B and D. We recover B and D through least squares.

3.1.5 Numerical Efficiencies by LQ Factorization

In the case where N is large, the construction of the matrix $Y_f \Pi_{U_f}^{\perp} Z^T$ in Eq. (3.8) and the subsequent calculation of its SVD are computationally intensive. Verhaegen has shown in [20] that from the following LQ decomposition

$$\begin{bmatrix} U_f \\ U_p \\ Y_p \\ Y_f \end{bmatrix} = \begin{bmatrix} L_{11} & 0 & 0 & 0 \\ L_{21} & L_{22} & 0 & 0 \\ L_{31} & L_{32} & L_{33} & 0 \\ L_{41} & L_{42} & L_{43} & L_{44} \end{bmatrix} \begin{bmatrix} Q_1 \\ Q_2 \\ Q_3 \\ Q_4 \end{bmatrix} \tag{3.16}$$

we have

$$\text{range}\left(\lim_{N\to\infty} \frac{1}{\sqrt{N}} \begin{bmatrix} L_{42} & L_{43} \end{bmatrix} \right) = \text{range}\left(\Gamma_f\right) \tag{3.17}$$

This shows an equivalency between Eq. (3.8) and Eq. (3.17), therefore we can estimate the column space of $\hat{\Gamma}_f$ by computing the LQ decomposition in Eq. (3.16), taking the SVD of the matrix $\begin{bmatrix} L_{42} & L_{43} \end{bmatrix}$, and reducing the system order as described above.

3.2 Closed-Loop Subspace Identification

In many real-world situations, it is either not practical or not possible to collect open-loop input and output data. An unstable system relying on some form of feedback control to operate safely is an example of such a case. It is well known that traditional subspace methods produce biased results in the presence of feedback. This is due to the correlation between the system input and past noise as the controller attempts to eliminate system disturbances [13], violating Assumption 4 introduced in the previous section. As a result, traditional SIMs are not albe to fully decouple the input and noise sequences when estimating the subspace of the extended observability matrix.

Recently, several new approaches to identifying closed-loop systems by decou-

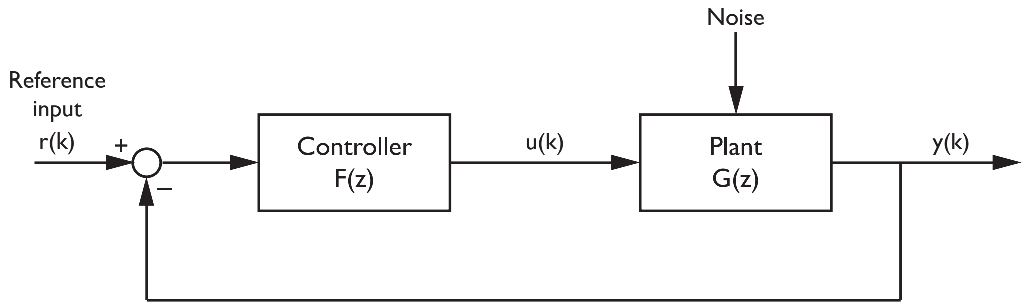

Figure 3.3: A block diagram of an LTI system operating under feedback control.

pling inputs from past noise (thus removing any bias) have been proposed. Among these approaches are the Innovation Estimation Method (IEM) proposed by Qin and Ljung [14] and the Whitening Filter Approach (WFA) proposed by Chiuso and Picci [3]. The IEM pre-estimates the innovation sequence E_f row-wise via a high-order Auto-Regression model with eXogeneous inputs (ARX) algorithm, which is then used to estimate Γ_f from the extended state space model. The WFA partitions a modified version of the extended state space model row-wise and estimates Γ_f through a multi-stage least squares followed by an SVD. It is worth noting that Chiuso and Picci concluded in [3] that while all closed-loop subspace identification algorithms considered produce somewhat biased results in the presence of feedback control, these algorithms are still able to provide significant improvements over traditional SIMs when identifying closed-loop systems.

We now present an overview of the IEM procedure to identify systems operating in closed loop. We assume the following to be true:

Assumption 1: The matrix $A - KC$ is stable (i.e. its eigenvalues lie strictly within the unit circle).

Assumption 2: The pair (A, C) is observable and $(A, [B \quad K])$ is observable.

Assumption 3: The innovation sequence $e(k)$ is zero-mean white noise.

Assumption 4: The input sequence $u(k)$ is persistently exciting.

3.2.1 Extended State Space Model

We again consider the combined deterministic-stochastic LTI system given in its innovation form as

$$x(k+1) = Ax(k) + Bu(k) + Ke(k) \tag{3.18a}$$

$$y(k) = Cx(k) + Du(k) + e(k) \tag{3.18b}$$

We now assume the system input sequence $u(k)$ is determined through feedback where

$$u(k) = F\big(r(k) - y(k)\big)$$

where $r(k)$ is the reference input. Based on the state space representation, an extended state space model can be formulated as

$$Y_p = \Gamma_p X_{k-p} + H_p U_p + G_p E_p \tag{3.19a}$$

$$Y_f = \Gamma_f X_k + H_f U_f + G_f E_f \tag{3.19b}$$

where p and f denote past and future horizons, respectively. The extended observability matrix is

$$\Gamma_f = \begin{bmatrix} C \\ CA \\ \vdots \\ CA^{f-1} \end{bmatrix}$$

and H_f and G_f are Toeplitz matrices of the Markov parameters of the deterministic and stochastic subsystems, respectively:

$$H_f = \begin{bmatrix} D & 0 & 0 & \cdots & 0 \\ CB & D & 0 & \cdots & 0 \\ CAB & CB & D & \cdots & 0 \\ \vdots & \vdots & \vdots & \ddots & \vdots \\ CA^{f-2}B & CA^{f-3}B & CA^{f-4}B & \cdots & D \end{bmatrix}$$

$$G_f = \begin{bmatrix} I & 0 & 0 & \cdots & 0 \\ CK & I & 0 & \cdots & 0 \\ CAK & CK & I & \cdots & 0 \\ \vdots & \vdots & \vdots & \ddots & \vdots \\ CA^{f-2}K & CA^{f-3}K & CA^{f-4}K & \cdots & I \end{bmatrix}$$

We arrange the input sequence into the following block Hankel form with k block rows and N columns:

$$U_p = \begin{bmatrix} u(0) & u(1) & \cdots & u(N-1) \\ u(1) & u(2) & \cdots & u(N) \\ \vdots & \vdots & \ddots & \vdots \\ u(k-1) & u(k) & \cdots & u(k+N-2) \end{bmatrix}$$

$$U_f = \begin{bmatrix} u(k) & u(k+1) & \cdots & u(k+N-1) \\ u(k+1) & u(k+2) & \cdots & u(k+N) \\ \vdots & \vdots & \ddots & \vdots \\ u(2k-1) & u(2k) & \cdots & u(2k+N-2) \end{bmatrix}$$

We construct similar matrices Y_p, Y_f, E_p, and E_f for the output and noise sequences. The state sequences are

$$X_k = \begin{bmatrix} x(k) & x(k+1) & \cdots & x(k+N-1) \end{bmatrix}$$

$$X_{k-p} = \begin{bmatrix} x(k-p) & x(k-p+1) & \cdots & x(k-p+N-1) \end{bmatrix}$$

3.2.2 Estimation of the Extended Observability Matrix with Innovation Estimation

The extended state space model is

$$Y_f = \Gamma_f X_k + H_f U_f + G_f E_f \tag{3.20}$$

If we partition the extended state space model row-wise, for the i^{th} row we have

$$Y_f = \begin{bmatrix} Y_{f1} \\ Y_{f2} \\ \vdots \\ Y_{ff} \end{bmatrix}, \qquad Y_{fi} = \Gamma_{fi} X_k + H_{fi} U_{fi} + G_{fi} E_{fi} \tag{3.21}$$

where the extended observability matrix is

$$\Gamma_f = \begin{bmatrix} \Gamma_{f1} \\ \Gamma_{f2} \\ \vdots \\ \Gamma_{ff} \end{bmatrix}, \qquad \Gamma_{fi} = CA^{i-1}$$

and the i^{th} rows of H_f and G_f are, respectively

$$H_{fi} = \begin{bmatrix} H_{i-1} & H_{i-2} & \cdots & H_1 & H_0 \end{bmatrix} = \begin{bmatrix} CA^{i-2}B & CA^{i-3}B & \cdots & CB & D \end{bmatrix}$$

$$G_{fi} = \begin{bmatrix} G_{i-1} & G_{i-2} & \cdots & G_1 & G_0 \end{bmatrix} = \begin{bmatrix} CA^{i-2}K & CA^{i-3}K & \cdots & CK & I \end{bmatrix}$$

Additionally, we define

$$H_{fi}^{-} = \begin{bmatrix} H_{i-1} & H_{i-2} & \cdots & H_1 \end{bmatrix} = \begin{bmatrix} CA^{i-2}B & CA^{i-3}B & \cdots & CB \end{bmatrix}$$

$$G_{fi}^{-} = \begin{bmatrix} G_{i-1} & G_{i-2} & \cdots & G_1 \end{bmatrix} = \begin{bmatrix} CA^{i-2}K & CA^{i-3}K & \cdots & CK \end{bmatrix}$$

and derive an equivalent representation of the partitioned state space model as

$$Y_{fi} = \Gamma_{fi} X_k + H_{fi}^{-} U_{i-1} + H_{f1} U_1 + G_{fi}^{-} E_{i-1} + E_{fi} \tag{3.22}$$

By letting $A_K = A - KC$ and $B_k = B - KD$, we are able to derive an expression for the unknown state sequence X_k by iterating Eq. (3.20)

$$X_k = L_p Z_p^T + A_K^p X_{k-p} \tag{3.23}$$

where

$$
\begin{aligned}
X_k &= \begin{bmatrix} x(k) & x(k+1) & \cdots & x(k+N-1) \end{bmatrix} \\
L_p &= \begin{bmatrix} L_p^y & L_p^u \end{bmatrix} \\
L_p^u &= \begin{bmatrix} A_K^{p-1}B_K & A_K^{p-2}B_K & \cdots & B_K \end{bmatrix} \\
L_p^y &= \begin{bmatrix} A_K^{p-1}K & A_K^{p-2}K & \cdots & K \end{bmatrix} \\
Z_p &= \begin{bmatrix} Y_p \\ U_p \end{bmatrix}
\end{aligned}
$$

Substituting Eq. (3.23) into Eq. (3.22) we have

$$Y_{fi} = \Gamma_{fi} L_p Z_p^T + \Gamma_{fi} A_K^p X_{k-p} + H_{fi}^- U_{i-1} + H_{f1} U_1 + G_{fi}^- E_{i-1} + E_{fi} \tag{3.24}$$

Recalling from Assumption 1, we require the eigenvalues of A_K to lie within the unit circle, so for a sufficiently large p, $A_K^p \approx 0$. Additionally, for convenience we assume there is no feedforward term (that is, $D = 0$) then $H_{f1} = 0$ so Eq. (3.24) simplifies to

$$Y_{fi} = \Gamma_{fi} L_p Z_p^T + H_{fi}^- U_{i-1} + G_{fi}^- E_{i-1} + E_{fi} \tag{3.25}$$

or equivalently in matrix form,

$$Y_{fi} = \begin{bmatrix} \Gamma_{fi} L_z & H_{fi}^- & G_{fi}^- \end{bmatrix} \begin{bmatrix} Z_p \\ U_{i-1} \\ E_{i-1} \end{bmatrix} + E_{fi} \tag{3.26}$$

Because the future innovation sequence E_{fi} is uncorrelated with the past innovation sequence E_{i-1}, instrumental variable matrix Z_p, and past output sequence U_{i-1} we see that Eq. (3.25) is formulated in such a way that we can estimate Γ_{fi} row-wise even when the system input and past noise are correlated (i.e. the system is operating with feedback). The only requirement is that future innovation be uncorrelated with past input, which is true for both a pen and closed-loop systems.

In order to estimate the innovation sequence E_f, we consider the first row of the extended state space model by setting $i = 1$ in Eq. (3.25):

$$Y_{f1} = \Gamma_{f1} L_p Z_p^T + E_1 \tag{3.27}$$

We are able to estimate the innovation term E_1 through the following least squares

$$\hat{E}_1 = Y_{f1} - \hat{\Gamma}_{f1} \hat{L}_p Z_p \tag{3.28}$$

with

$$\hat{\Gamma}_{f1} \hat{L}_p = Y_{f1} Z_p^{\dagger} \tag{3.29}$$

In the more general case for $i = 1, 2, \ldots, f$ we have

$$\hat{E}_i = \begin{bmatrix} \hat{E}_{f1} \\ \hat{E}_{f2} \\ \vdots \\ \hat{E}_{f1} \end{bmatrix} = \begin{bmatrix} \hat{E}_{i-1} \\ \hat{E}_{fi} \end{bmatrix} \tag{3.30}$$

thus using Eqs. (3.25) and (3.30) we are able to estimate the innovation sequence recursively using the system input-output data. Once the innovation sequence is known, we are able to estimate the unknown coefficient matrices through least squares as follows:

$$\begin{bmatrix} \hat{\Gamma}_{fi} \hat{L}_p & \hat{H}_{fi}^{-} & \hat{G}_{fi}^{-} \end{bmatrix} = Y_{fi} \begin{bmatrix} Z_p \\ U_{i-1} \\ \hat{E}_{i-1} \end{bmatrix}^{\dagger} \tag{3.31}$$

Computing the least squares estimate of $\hat{\Gamma}_{fi} \hat{L}_z$ row by row using Eq. (3.31), we obtain an estimate of the full matrix $\hat{\Gamma}_f \hat{L}_p$

$$\hat{\Gamma}_f \hat{L}_p = \begin{bmatrix} \hat{\Gamma}_{f1} \\ \hat{\Gamma}_{f2} \\ \vdots \\ \hat{\Gamma}_{ff} \end{bmatrix}$$

from which am estimate of the column space of the extended observability matrix can be obtained via an SVD where

$$\hat{\Gamma}_f = US^{1/2} \tag{3.32}$$

We follow the same procedure outlined in Section 3.1.3 to reduce the rank of the identified system, and recover estimates of the system matrices as in Section 3.1.4

Results from ¡CITE HERE¿ have shown a reduction in bias when identifying systems operating in closed-loop using IEM over traditional SIMs (CVA, N4SID, MOESP). Also, comparisons between the IEM and other closed-loop PEM and subspace identification techniques have shown that under the stated assumptions, estimation differences between the IEM and others are minimal and the IEM provides a consistent system estimate.

CHAPTER 4

Approach

4.1 Quadrotor Platform

Because the design and construction of a quadrotor is beyond the scope of this project, we will use a commercially available vehicle called the Bitcraze Crazyflie [1]. The Crazyflie, shown in Figure 4.1 is a small, low cost, open-source quadrotor kit suitable for indoor flight. It measures 9 cm motor to motor and weighs 19 grams. A 170 mAh lithium-polymer battery powers the vehicle, providing 7 minutes of flight time. An onboard microcontroller is responsible for vehicle stabilization and control and reads sensor measurements from a three-axis accelerometer and a three-axis gyroscope.

Figure 4.1: Bitcraze Crazyflie Quadrotor

Vehicle pitch, roll, yaw, and thrust inputs are set in one of two ways. First, a USB gamepad connected to a computer running the Crazyflie PC client provides a method for direct user control of the vehicle. Second, the PC client exposes a Python API, making it possible to programmatically send the vehicle control set-points. The vehicle receives control inputs and transmits telemetry data wirelessly over a 2.4 GHz radio connection to a USB radio dongle connected to the Crazyflie PC client running on a laptop computer.

The onboard stabilization and control system implements an outer-loop attitude controller and an inner-loop rate controller, as shown in Figure 4.2. Reference pitch and roll commands (ϕ and θ, respectively) are fed to the attitude controller (outputting desired rates) and reference yaw rate ($\dot{\psi}$) is fed directly to the rate controller. The inner-loop rate control operates at 500 Hz and the outer-loop attitude control operates at 250 Hz.

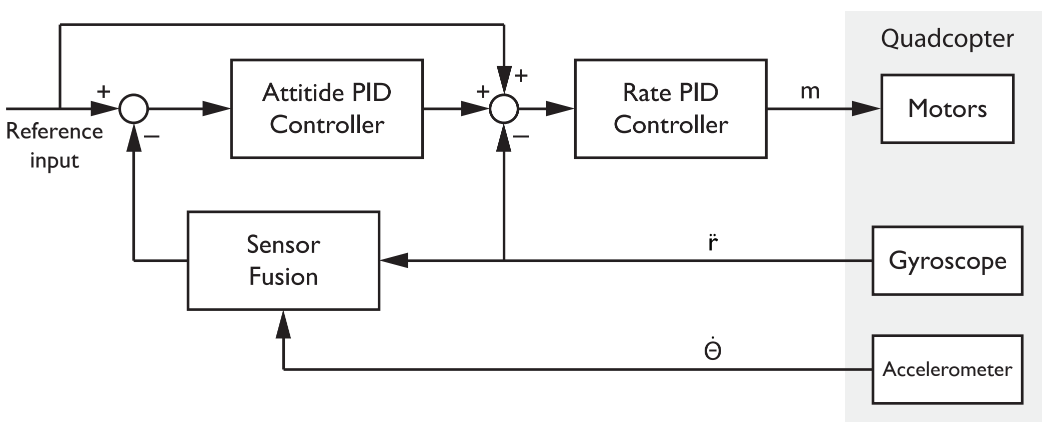

Figure 4.2: Crazyflie stabilization and control system block diagram where $m = \begin{bmatrix} m_1 & m_2 & m_3 & m_4 \end{bmatrix}^T$ is a vector of motor commands, $\ddot{r} = \begin{bmatrix} \ddot{x} & \ddot{y} & \ddot{z} \end{bmatrix}^T$ is a vector of inertial-frame accelerations, and $\dot{\Theta} = \begin{bmatrix} \dot{p} & \dot{q} & \dot{r} \end{bmatrix}^T$ is a vector of inertial-frame angular rotation rates.

4.2 Experiment Design

A crucial step in system identification is experiment design. In order to develop a robust system model, the input sequence must sufficiently excite all system modes to be identified and the sensor data must be sampled fast enough to avoid aliasing. Because the choices made during experiment design have a direct impact on the identified model, it may be necessary to update aspects of the design if the model is found to be insufficient. In this sense, the development of a system model through system identification may be viewed as an iterative procedure.

4.2.1 Input Design

The input sequence plays an important role in system identification by providing a mechanism by which the unknown system is excited, allowing us to capture system input-output data required by the identification problem. Common input sequences used for system identification include impulse signals, doublets, white noise sequences, frequency sweeps, and pseudo-random binary sequences [22]. We considered three major factors when selecting an input sequence:

1. The sequence must be capable of sufficiently exciting all system modes to be identified.
2. The sequence must set the persistence of excitation criteria established in Assumption 4 in Section 3.2.
3. The sequence must be either simple enough to manually execute or formatted in such a way that it is easily transmitted to the vehicle for execution.

Considering the above factors, we chose to use the pseudo-random binary sequence (PRBS) as system input. A PRBS signal, shown in Figure 4.3, is persistently exciting to the order of the period of the signal [24] and is easily transmitted to the Crazyflie quadcopter by sending input sequences through the Python API.

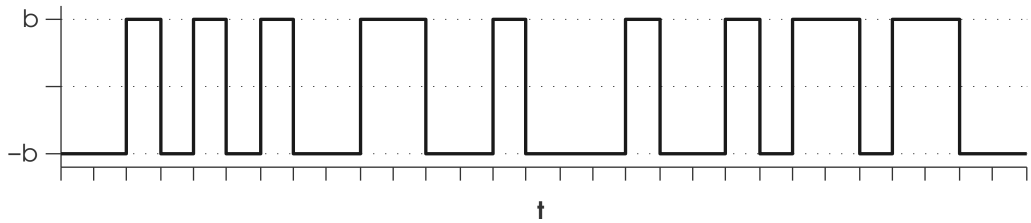

Figure 4.3: A general Pseudo-Random Binary Sequence (PRBS).

We generated the PRBS signals used for identification by using MATLAB's System Identification Toolbox. Signals were generated for pitch, roll, and yaw rate. Additional input conditioning was performed to appropriately scale the magnitude of the input signal. Scaling factors were experimentally determined to sufficiently excite the vehicle without rendering it uncontrollable.

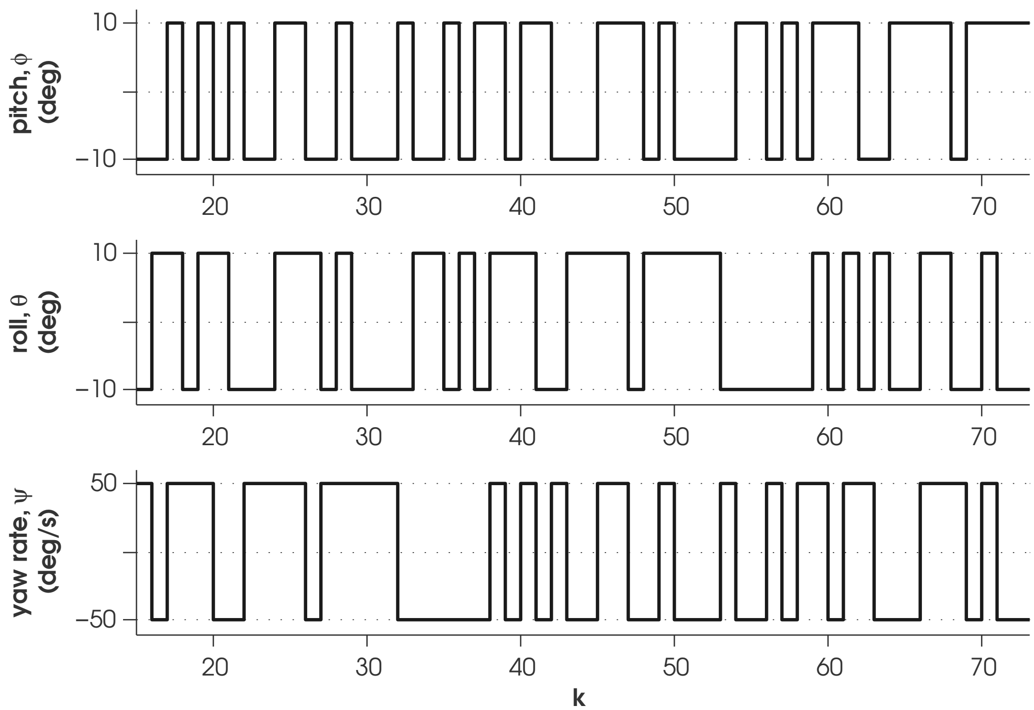

Figure 4.4: A sample PRBS signal used for identification showing scaled inputs for vehicle pitch = ±10°, roll = ±10°, and yaw rate = ±50°/sec.

Because the Python API requires system input sequences to be formatted as {pitch, roll, yaw rate, thrust}, we also experimentally determined a thrust input which results in vehicle hover. The general flight test sequence is: vehicle power on and sensor calibration, take off and hover, free flight under PRBS input, test conclusion.

FIGURE

Talk about how PRBS goes into controller which in turn generates motor commands

4.2.2 Data Collection

4.3 Data Analysis

INCLUDE OVERVIEW OF IEM ALGORITHM IN BOX (MATH-BASED) IN THIS SECTION

4.3.1 Data Preprocessing

4.3.2 Model Identification

4.4 Verification

CHAPTER 5

Results

CHAPTER 6

Conclusion

6.1 Future Work

References

[1] Bitcraze. http://www.bitcraze.se, 2013.

[2] Anthony RS Bramwell, David Balmford, and George Done. *Bramwell's helicopter dynamics*. Butterworth-Heinemann, 2001.

[3] Alessandro Chiuso and Giorgio Picci. Consistency analysis of some closed-loop subspace identification methods. *Automatica*, 41(3):377–391, 2005.

[4] Shweta Gupte, Paul Infant Teenu Mohandas, and James M Conrad. A survey of quadrotor unmanned aerial vehicles. In *Southeastcon, 2012 Proceedings of IEEE*, pages 1–6. IEEE, 2012.

[5] Gabriel M Hoffmann, Haomiao Huang, Steven L Waslander, and Claire J Tomlin. Quadrotor helicopter flight dynamics and control: Theory and experiment. In *Proc. of the AIAA Guidance, Navigation, and Control Conference*, pages 1–20, 2007.

[6] Magnus Jansson. On subspace methods in system identification and sensor array signal processing. *These de doctorat-Royal institute of technology, Stockholm*, 1997.

[7] Rudolph Emil Kalman et al. A new approach to linear filtering and prediction problems. *Journal of basic Engineering*, 82(1):35–45, 1960.

[8] Tohru Katayama. *Subspace methods for system identification*. Springer, 2005.

[9] Arda Özgür Kivrak. Design of control systems for a quadrotor flight vehicle equipped with inertial sensors. *Atilim University, December*, 2006.

[10] Wallace E Larimore. Canonical variate analysis in identification, filtering, and adaptive control. In *Decision and Control, 1990., Proceedings of the 29th IEEE Conference on*, pages 596–604. IEEE, 1990.

[11] Daniel Mellinger, Michael Shomin, and Vijay Kumar. Control of quadrotors for robust perching and landing. In *Proc. Int. Powered Lift Conf*, pages 119–126, 2010.

[12] Nathan Michael, Daniel Mellinger, Quentin Lindsey, and Vijay Kumar. The grasp multiple micro-uav testbed. *Robotics & Automation Magazine, IEEE*, 17(3):56–65, 2010.

[13] S Joe Qin. An overview of subspace identification. *Computers & chemical engineering*, 30(10):1502–1513, 2006.

[14] S Joe Qin and Lennart Ljung. Closed-loop subspace identification with innovation estimation. In *Proceedings of SYSID*, volume 2003, 2003.

[15] Zak Sarris and STN ATLAS. Survey of uav applications in civil markets (june 2001). In *The 9 th IEEE Mediterranean Conference on Control and Automation (MED'01)*, 2001.

[16] Torsten Söderström and Petre Stoica. *Instrumental variable methods for system identification*, volume 161. Springer-Verlag Berlin, 1983.

[17] Kimon P Valavanis. *Advances in unmanned aerial vehicles: state of the art and the road to autonomy*, volume 33. Springer, 2007.

[18] Peter Van Overschee and Bart De Moor. N4sid: Subspace algorithms for the identification of combined deterministic-stochastic systems. *Automatica*, 30(1):75–93, 1994.

[19] Peter Van Overschee and Bart De Moor. A unifying theorem for three subspace system identification algorithms. *Automatica*, 31(12):1853–1864, 1995.

[20] Michel Verhaegen. Identification of the deterministic part of mimo state space models given in innovations form from input-output data. *Automatica*, 30(1):61–74, 1994.

[21] Michel Verhaegen and Patrick Dewilde. Subspace model identification part 1. the output-error state-space model identification class of algorithms. *International journal of control*, 56(5):1187–1210, 1992.

[22] Michel Verhaegen and Vincent Verdult. *Filtering and system identification: a least squares approach*. Cambridge university press, 2007.

[23] Mats Viberg. Subspace-based methods for the identification of linear time-invariant systems. *Automatica*, 31(12):1835–1851, 1995.

[24] Stacy S Wilson. Understanding the prbs signal as an optimum input signal in the wavelet-correlation method of system identification using multiresolution analysis. In *SoutheastCon, 2005. Proceedings. IEEE*, pages 39–44. IEEE, 2005.